

## Transformation of the Three-Phase Interlines During the Electrochemical Deoxidation of TiO<sub>2</sub>

Pingsheng Lai, Meilong Hu<sup>\*</sup>, Zhengfeng Qu, Leizhang Gao, Chenguang Bai, Shengfu Zhang

College of Materials Science and Engineering, Chongqing University, Chongqing 400044, China

\*E-mail: [hml@cqu.edu.cn](mailto:hml@cqu.edu.cn)

*Received:* 28 December 2017 / *Accepted:* 6 March 2018 / *Published:* 10 April 2018

---

The deoxidation of TiO<sub>2</sub> cathode in molten CaCl<sub>2</sub> was studied at 900 °C and under 3.2 V for different time periods. Materials were characterized before and after electrolysis by scanning electron microscopy, X-ray energy dispersive spectroscopy, and X-ray diffraction. The results show that the deoxidation process invariably proceeded through several intermediate species and can be described as four steps. The formation of the interfaces, especially the three-phase interlines (3PI) between the formed intermediate species and its subsequent transformation during the deoxidation process, are discussed. These findings are compared to the previous typical 3PI model.

---

**Keywords:** three-phase interline, electrochemical deoxidation, titanium dioxide, calcium chloride

### 1. INTRODUCTION

The invention of electro-deoxidation has produced a large body of research in recent years [1], largely owing to its use as a cost-effective process for extracting metals from their solid oxides, which is normally named FFC–Cambridge process. Examples include silicon [2, 3], titanium [4-6], tantalum [7, 8], chromium [9, 10], uranium [11, 12], and ferrum [13, 14]. Titanium is especially important due to its extensive usage in chemical industry, aerospace engineering, medical science, sports equipment and so on. Unfortunately, the present commercial production of titanium by the Kroll process is lengthy and labor-intensive, which involves high costs and limits its widespread use in many applications. Therefore, many studies have been carried out to investigate the mechanism of the electro-reduction of the process and to thereby modify the FFC process.

Molten salt electrolysis as a new alternative method has a variety of advantages such as simplicity of process and low cost among others. Therefore, many investigations have been carried out to explore the mechanism of the electro-reduction of the titanium dioxides in molten salts. Initial studies of the process for the reduction of the titanium dioxide proposed that the electro-reduction of

the sample occurs directly with transformation of titanium dioxide to titanium [4, 6, 15-17]. For example, Chen determined a reaction path way of  $\text{TiO}_2 \rightarrow \text{Ti}_2\text{O}_3 \rightarrow \text{TiO} \rightarrow \text{Ti}$  [15]. K. Dring proposed that  $\text{Ti}_3\text{O}_5$  exists during the electrochemical reduction of titanium dioxide in molten calcium chloride, so the kinetic pathway should be  $\text{TiO}_2 \rightarrow \text{Ti}_3\text{O}_5 \rightarrow \text{Ti}_2\text{O}_3 \rightarrow \text{TiO} \rightarrow \text{Ti}$  [18]. Subsequently, Schwandt indicated that reduction proceeds through several individual stages, some of which involve the formation and decomposition of calcium titanates, which can be expressed as  $\text{TiO}_2 \rightarrow \text{CaTiO}_3 + \text{Ti}_x\text{O}_y \rightarrow \text{CaTi}_2\text{O}_4 \rightarrow \text{TiO} \rightarrow \text{Ti}$  [19-21]. Further analysis revealed a more complex reaction pathway. However, these studies didn't focus on the phase transformation and the interface migration during the whole process.

In this study, the partially reduced titanium dioxide pellets used to establish the reaction pathway were further investigated, applying a range of analysis techniques to further understand the reaction pathway and the phase transition during the electro-reduction process. In addition, comparing to the classic three-phase interline theory, we found that the deoxidation process of titanium dioxide is a bit different from the other metal oxides. Therefore, the electro-reduction behavior and the interface migration of titanium dioxide were investigated.

## 2. EXPERIMENTAL PROCEDURE

In this work,  $\text{TiO}_2$  (99%, analytical grade, Kelong Chemical Reagent Factory, Chengdu China) powder was selected as the oxide precursor. The titanium dioxide was uniaxially pressed in a hydraulic press with ~6–7 MPa of pressure to produce pellets with 10 mm in diameters and 15 mm in thicknesses. These pellets (about 1.4 g) were subsequently sintered at 900 °C in atmospheric air for 2 h and cooled to the room temperature. The pellets were fully wrapped by molybdenum wire for good electrical contact.

The electro-deoxidization experiment includes the pretreatment of the calcium chloride and the electrochemical reduction process. The pre-treatment process involved the thermal drying of the solid calcium chloride and the pre-electrolysis of the molten calcium chloride. The solid molten salt was dried in an oven at ~100 °C for 2 h and 300 °C for 3 h to remove physical water and crystal water, respectively. Electrochemical reduction experiments were carried out in a dense alumina crucible with a 100 mm internal diameter and 100 mm height, which was dried at 150 °C before the experiment. A previously prepared pellet was attached to the molybdenum rod which served as the cathode, and a graphite rod served as the anode. The interior of the sealed reactor was vacuated and then flushed with dry argon continuously. Pre-electrolysis was carried out at 850 °C for 2 h with 2 V to remove water and impurities in the pellets. The reactor was then heated at a constant rate of 3 °C/min by the furnace with an argon flow of 120 mL/min until the target temperature (900 °C) was reached. A schematic diagram of the electrolytic apparatus is shown in Fig. 1.

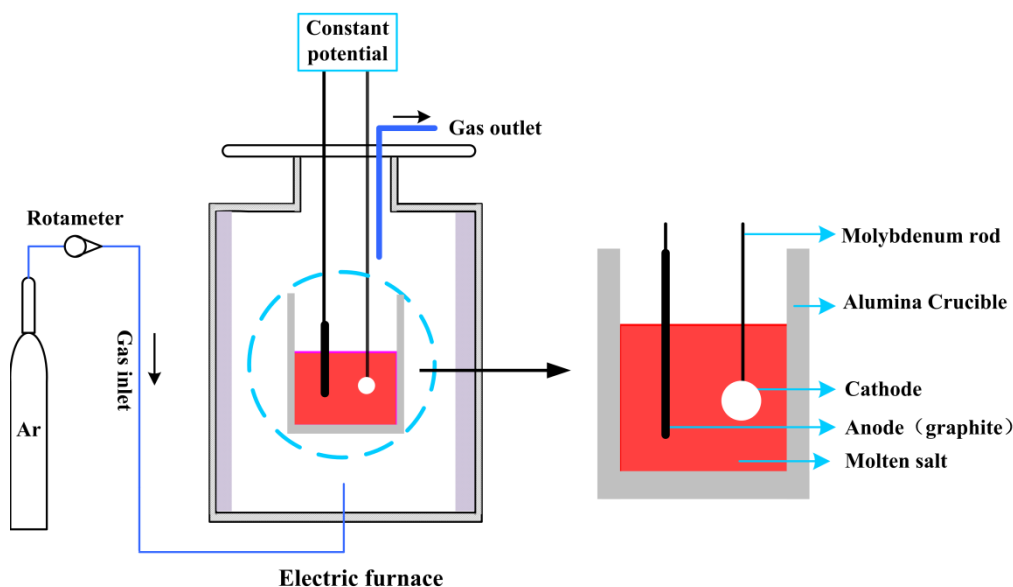


**Figure 1.** Schematic diagram of the electrolytic apparatus.

When the current of the pre-electrolysis was kept at a constant value, we assumed that the impurities in the molten salt were removed. Thereafter, the sintered titanium dioxide pellet was slowly immersed into the electrolyte, and the graphite rod was then immersed to the molten salt. A constant voltage of 3.2 V was applied between the anode and the cathode. The electrolysis of the pellets was terminated after 6 h, 8 h, 12 h, 14 h, 18 h, and 24 h. After electrolyzing, the electrodes were raised out of the electrolyte, and then cooled to room temperature in the reactor. The pellets were placed into distilled water and then cleaned by an ultrasonic cleaner to remove the electrolyte. The morphology and elements distribution of the pellets were observed by scanning electron microscopy (SEM, TESCAN VEGA III) and X-ray energy-dispersive spectroscopy (EDS, Oxford INCA Energy 350) operated at 20.0 keV, respectively. The phase composition was analyzed by X-ray diffraction (XRD, RigakD/Max-2500).

### 3. RESULTS AND DISCUSSION

#### 3.1. Phase composition and microstructure after electrolysis

The macro photos of the pellets section after being electrolyzed in  $\text{CaCl}_2$  molten salt for different times are shown in Fig. 2. From Fig. 2, we observe that the sample becomes shinier as the electrolysis time increased. This indicates that the metallic phase increases with increasing electrolysis time. In addition, the pellets electrolyzed for 6 h and 8 h may only be partially electrolyzed. The 6 h sample especially no obvious shiny phase, and the phase composition was introduced later. Figure 3 shows the cross-sectional SEM images and EDS results of the  $\text{TiO}_2$  sample after electrolyzing in  $\text{CaCl}_2$  molten salt for 8 h. these shows that the sample predominantly consists of titanium (on the edge) and  $\text{TiO}_x$  (at the center), which reveals that the pellet at the surface was reduced more than those in the

bulk. The morphology of the metallic titanium in the pellets was observed by SEM in Fig. 4, demonstrating that the metallic particles are micro-sized and connects to each other. Moreover, the pellets electrolyzed for 12 h and longer were predominantly reduced to titanium, as observed by analyzing the EDS results, not displayed.

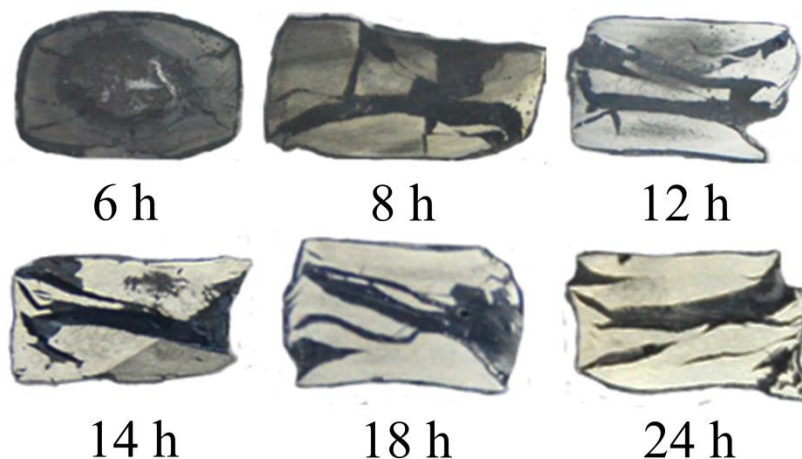


**Figure 2.** Macro photos of TiO<sub>2</sub> pellets section after electrolyzing in CaCl<sub>2</sub> molten salt for different times at 900 °C.

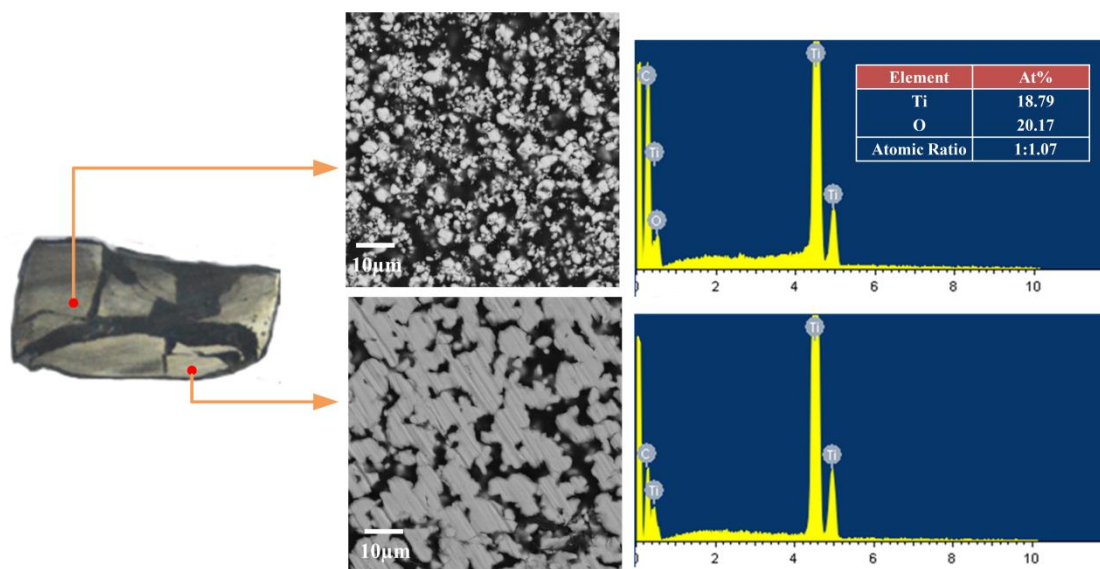


**Figure 3.** Scanning electron microscopic images and EDX results of the sample (1.4 g of the TiO<sub>2</sub> pellets) after electrolysis in CaCl<sub>2</sub> molten salt for 8 h at 900 °C.

Our attention was drawn to the pellets electrolyzed for 6 h, which were partially electro-reduced and could reveal the different phase compositions inside and out. Figure 5 shows the XRD patterns of the surface and interior of the TiO<sub>2</sub> pellet electrolyzed in CaCl<sub>2</sub> molten salt for 6 h. It is obvious that the pellet can be divided into different layers, whose phase compositions may be quite different. To compare the differences of the phase compositions between the adjacent layers, four layers of the pellet were defined in the SEM image, as shown in Fig. 6. Using surface energy spectrum

analysis and point energy spectrum analysis (Fig. 6) of the different layers, the phase compositions of the different layers were obtained and are shown in Table 1.

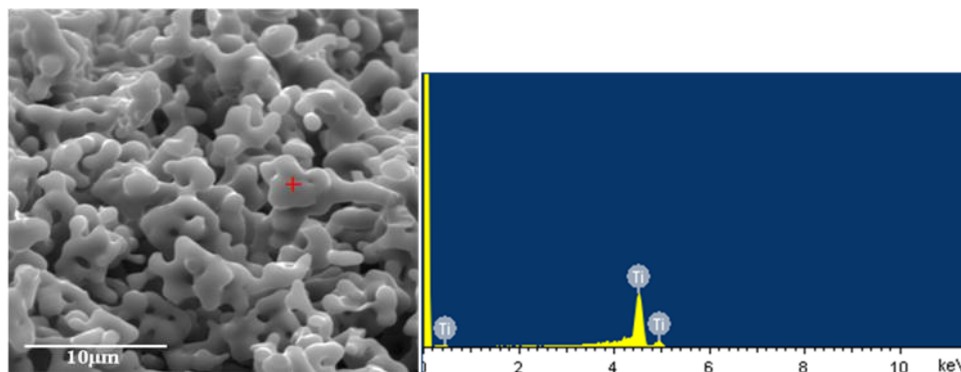


**Figure 4.** The morphology of the metallic Ti in figure 3, observed by scanning electron microscope.

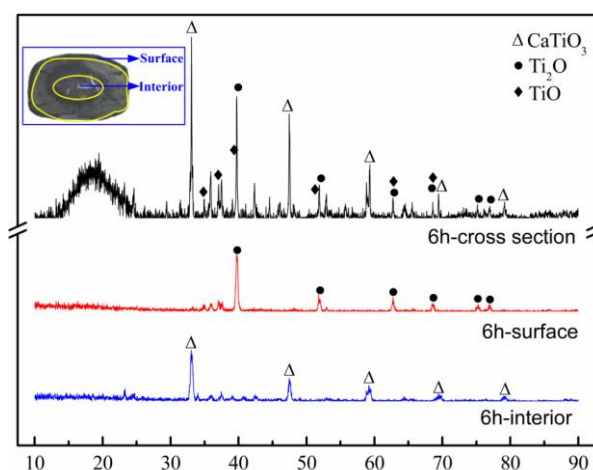


**Figure 5.** XRD patterns of the TiO<sub>2</sub> pellet section (both of surface and interior) after electrolyzing for 6 h in molten CaCl<sub>2</sub>.

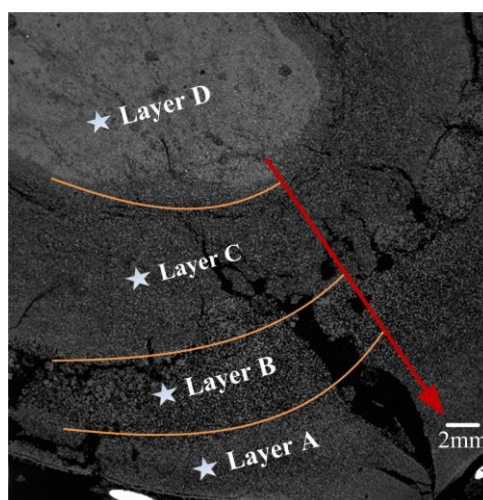


**Figure 6.** SEM image of a detail of the transformation in a section of the sample electrolyzed for 6 h.



**Table 1.** Phase composition of different layers

Layer	Phase Composition
A	TiO, Ti <sub>2</sub> O
B	TiO <sub>y</sub>
C	TiO <sub>x</sub> , CaO
D	CaTiO <sub>3</sub> , TiO <sub>x</sub> , CaO

Note:  $1 < y \leq x < 2$

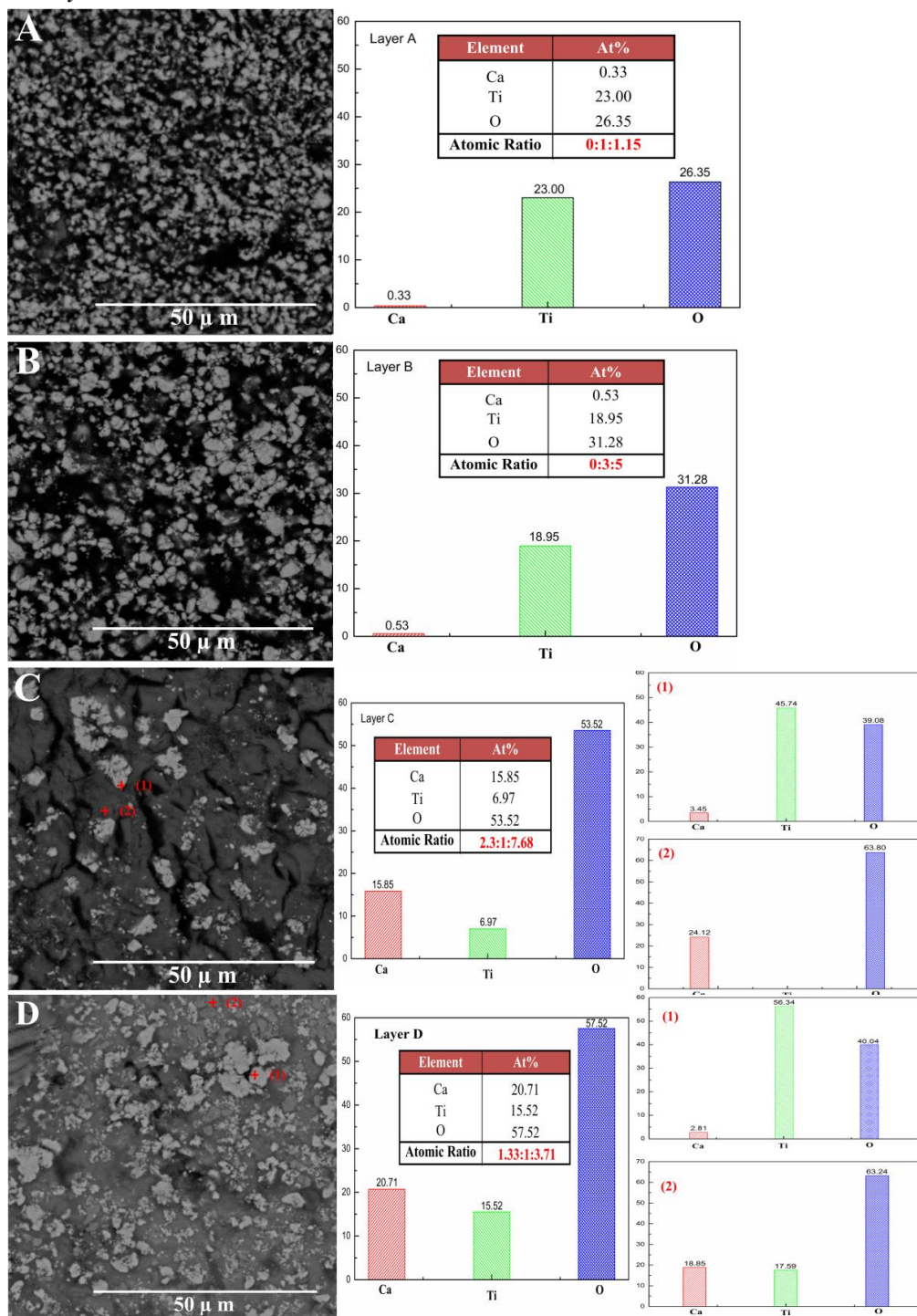


**Figure 7.** SEM images of different layers in figure 6 and EDX spectrum of the surface and spot scans of the corresponding images.

Figure 7 shows the images of surface scanning and the atomic ratios of the different layers of the sample. These data reveals that the pellet is partially reduced and that the oxygen content increased from outside to the inside, which indicates that the electro-deoxidation of the titanium dioxide occurs from the outside in. The surface of the sample electro-reduced for 6 h is entirely covered by a crust of Ti-O (layer A). A thin layer of titanium suboxides  $\text{TiO}_y$  ( $1 < y \leq x < 2$ ) (layer B) is also found, whose band is further towards the center of the pellet. Subsequently, the bulk of the sample remains a mixture of high—order Magneli phases and CaO (layer C). Toward the center, another relatively dense layer is found, consisting of  $\text{CaTiO}_3$  mixed with  $\text{TiO}_x$  (layer D).

Based on these results, it is reasonable to assume that the electro-reduction of titanium dioxide is a complicated process that contains a variety of intermediate products during the electrolysis. This agrees well with the established literature that the electro-reduction of  $\text{TiO}_2$  in molten calcium chloride occurs via the formation and decomposition of perovskite phase and titanium suboxides. This can be divided into several steps. In the beginning, the calcium ion and electron transfer to the interior of the pellet, and the titanium dioxide releases partial oxygen as  $\text{O}^{2-}$  which reacts with the calcium ion. Subsequently,  $\text{CaTiO}_3$  is generated and  $\text{TiO}_x$  remains. However, with continuation of charge, the  $\text{CaTiO}_3$  is gradually electrolyzed to form titanium suboxides, since the decomposition potential of  $\text{CaTiO}_3$  is relatively negative. Repeatability and reproducibility studies showed the same results, revealing that  $\text{CaTiO}_3$  is an inevitable intermediate product and will be further electrolyzed to form titanium suboxides during the electrolysis process. Finally, the titanium suboxides are further electrolyzed to TiO and, ultimately, to titanium.

C.Schwandt and D.J. Fray [19] have proposed the pathway in the electrochemical reduction of  $\text{TiO}_2$ . By analyzing partially reduced samples at different times, it was concluded that the electro-deoxidation of  $\text{TiO}_2$  is taking place in four stages. At first,  $\text{TiO}_2$  reacts with  $\text{Ca}^{2+}$  to produce titanium suboxides and  $\text{CaTiO}_3$ . These suboxides are then reduced to TiO by the action of  $\text{Ca}^{2+}$ , with more  $\text{CaTiO}_3$  produced as a by-product. Chemical reaction then occur between TiO and  $\text{CaTiO}_3$ , and a lower valent  $\text{CaTi}_2\text{O}_4$  is produced. In the final stage,  $\text{CaTi}_2\text{O}_4$  is electrochemically reduced to TiO, which will be further reduced to Ti. R. Bhagat [17] used white beam synchrotron XRD to characterize the phase that form in situ during the electrochemical reduction of  $\text{TiO}_2$ . It is found that  $\text{TiO}_2$  becomes sub-stoichiometric very early in reduction, facilitating the ionic conduction of O ions, that  $\text{CaTiO}_3$  persists to nearly the end of the process and that, finally, CaO forms just before completion of the process. However, in the terms of our inference, the  $\text{CaTiO}_3$  only formed by reaction between  $\text{TiO}_2$  and electrolyte, which is accord with the investigates by Bahgat and K. Dring [18], while the appearance of CaO in the initial time is different with the Bahgat's results which inferred that CaO just appears at the final stage of deoxidation of  $\text{TiO}_2$  due to the limited dissolution of CaO in molten salt.

### 3.2. Current versus time curves

Figure 8 shows the current versus different electrolytic time curves. It shows that the current, after reaching a peak value originally, drops down rapidly within short time, and then changes slowly. The current of 24 h dropped straightly at about 1.5 h, may caused by the experimental operations,

which makes it a little different to the others. The current versus time curves have been recorded by many investigators because it can reflect the behavior of electro-reduction process. The feature of curves are almost consistent with each other in the literature [16, 19, 21-22]. At the beginning of the electrolysis, the electro-deoxidization is carried mainly through electrochemical reaction, which starts at the “point” linked to the collector/titanium dioxide/electrolyte.  $\text{Ca}^{2+}$  ions transfer into the titanium dioxide cathode from the molten salt, electrons are provided to the cathode by current lead, and oxygen releases to the electrolyte from the titanium dioxide cathode, leading to the formation of titanium suboxides. As the titanium suboxides are electronic conductors, the cathode becomes conductive very shortly after reduction has commenced. The reduction is then no longer confined by the “points” of contact between the three phases but may occur over the entire interface of cathode and electrolyte. This process can primarily explain the phenomena that current rises rapidly in the initial stage. Due to the poor conductivity of  $\text{CaTiO}_3$  and suboxides, the current drops sharply. Owing to the extremely high binding energy between the O and Ti in titanium suboxides, the removal of oxygen in titanium suboxides takes a long time. At this stage, the current is at a small value and keep steady.

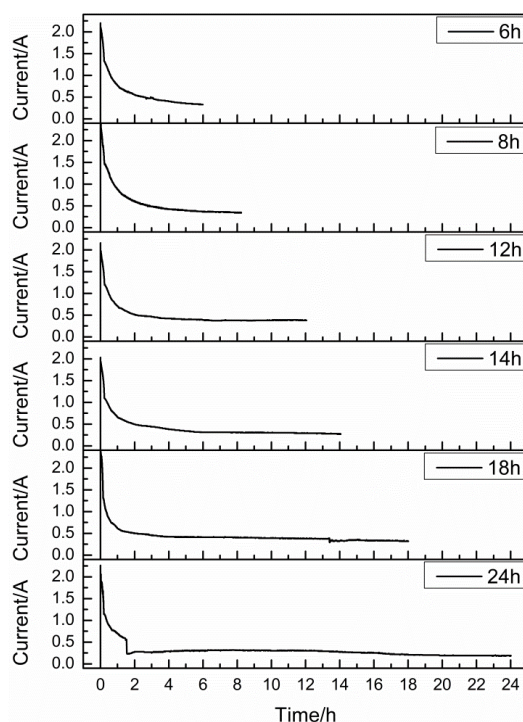


**Figure 8.** Current versus time curves obtained during electro-deoxidation experiments (1.4 g of  $\text{TiO}_2$  pellets,  $\text{CaCl}_2$  molten salt,  $900\text{ }^\circ\text{C}$ , 3.2 V).

### 3.3. Transformation of the three-phase interline

It can be concluded that the electro-deoxidization of the titanium dioxide proceeds from the outside in, by analyzing the electrolysis results at different times. However, the electrolytic mechanism has been found to be complex. A possible explanation was found from experimental observations



indicating that, for the reduction of oxide pellets or plates, the reduction always starts at the three-phase interline (3PI) [2, 9, 23, 24].

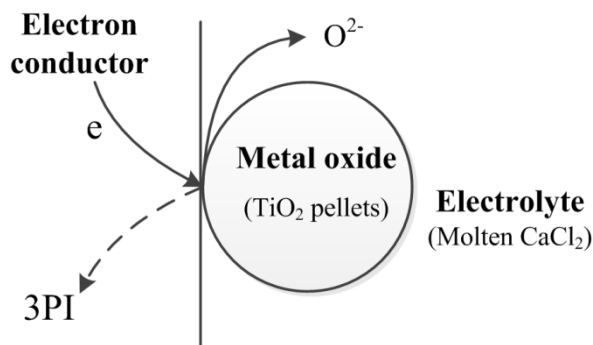


**Figure 9.** Electron and oxygen ion transfer at the metal/oxide/electrolyte three phase interline.

These observations led to the speculation that the reduction occurs through electron-transfer at the metal/oxide interface, but the oxygen ion transferred at the oxide/electrolyte interface, and the two interfaces are connected to the 3PI, as shown in Fig. 9 [23]. There are two pieces of evidences supporting this analysis. First, the phase change always occurs at the surface when metal oxide pellets are electrolyzed even for a short time. Second, because the total rate of charge transfer or current flow is proportional to the length of the 3PI (analogous to the current being proportional to the area of the electrode/electrolyte interface), the current flow in the beginning of the electrolysis is expected to gradually reach a maximum in cases where the initial metal/oxide contact area is small, which is described exactly in Fig. 8.

Three-phase electrochemistry is first proposed to explain the electro-reduction of silicon, chloride, thallium, etc., from their respective solid oxides in molten calcium chloride, and the successful reduction of  $\text{SiO}_2$  is strong evidence for this argument [2, 9]. However, upon further study, it is revealed that in many of the metal oxides, such as titanium and tantalum, both the oxygen diffusion in the solid phase and the effects of the electrolyte, occurring in the electro-reduction process, can contribute to generating the intermediate products. Thus, a multiphase (metal oxide, intermediates, metal, electrolyte) transformation exists in the electrolytic process instead of oversimplified three phases. In other words, there exist several interlines during the electrochemical reduction of titanium dioxide. The First is the earliest formed perovskite linking with the neighboring unreacted titanium dioxide, i.e., titanium dioxide/perovskite/electrolyte. Subsequently, the perovskite phase is electrolyzed to titanium suboxides, resulting in the three-interline of perovskite/titanium suboxides/electrolyte. Then, the conversion between suboxides and TiO occurs, leading to the three-interline of suboxides/TiO/electrolyte. Finally, the TiO discharges oxygen and changes to titanium, bringing about the TiO/titanium/electrolyte three-interline. As mentioned before, the 3PI results from the conversion between the two-solid phase. The reduction of the solid oxide begins at the 3PI of the current collector (metal or conductive metal oxides), oxide, and molten salt, and converts the solid oxide in direct contact with the current collector to the metal. At the same time, the oxygen in the oxide is ionized and enters the electrolyte. Thus, further reduction of the oxide can proceed at the 3PI connecting the newly

formed metal with the oxide and electrolyte, leading to the continuous movement of the 3PI. Comparing this to the illustration of the 3PI model, the most significant difference between the first three three-interlines and the 3PI is the two solid phases in the three-phase interlines, including titanium dioxide/perovskite/electrolyte, perovskite/titanium suboxides/electrolyte and titanium suboxides/TiO/electrolyte.

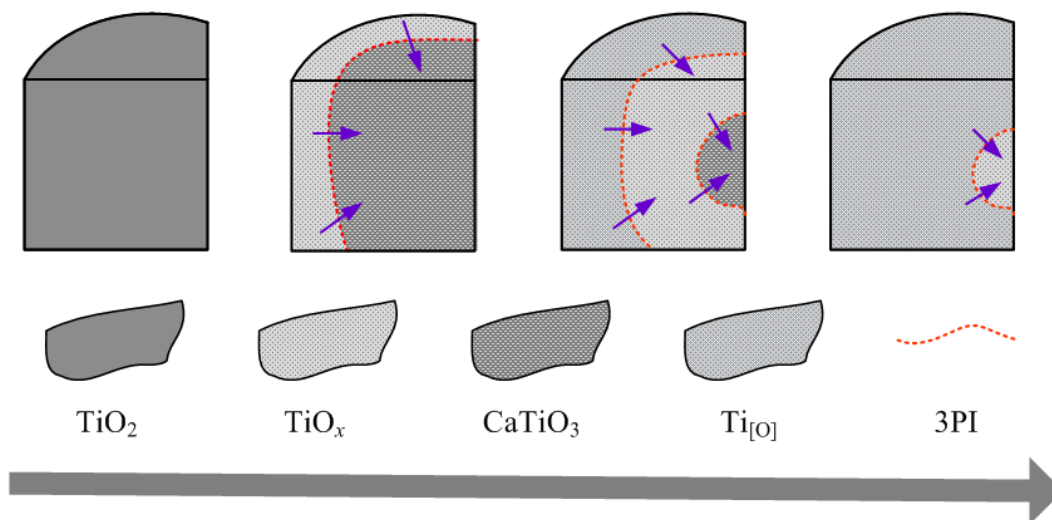


**Figure 10.** Schematic showing the transformation of the three-phase interlines during the electrolysis of  $\text{TiO}_2$  in  $\text{CaCl}_2$  molten salt.

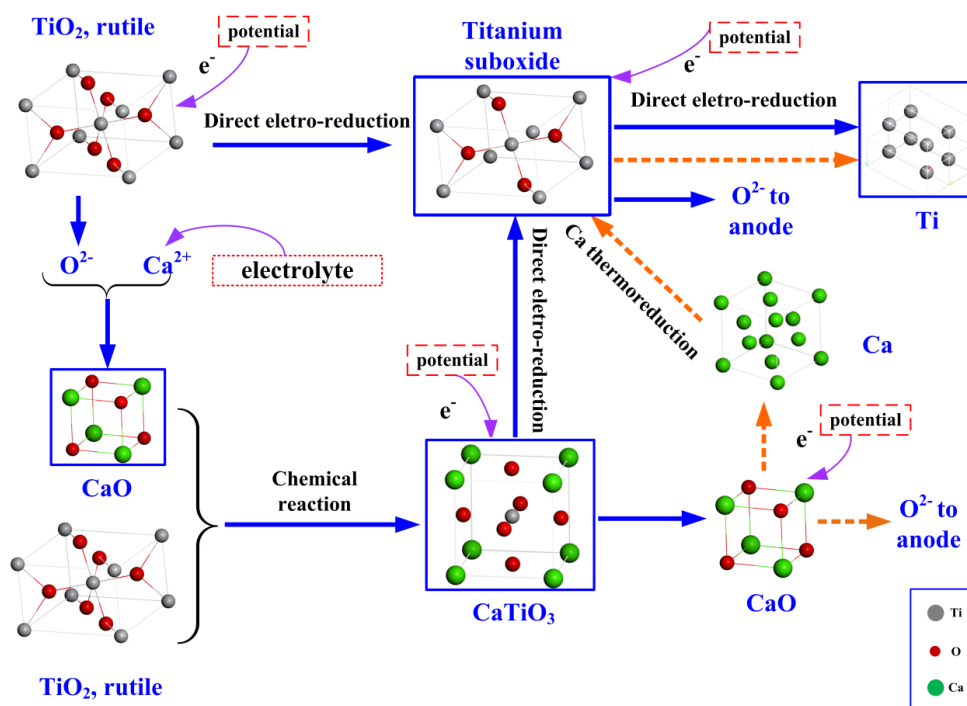


**Figure 11.** Schematic diagram visualizing the phase transition during the whole electro-reduction of a  $\text{TiO}_2$  pellets electrode in  $\text{CaCl}_2$  molten salt.

Both of two solid phases can obtain electrons and discharge oxygen ions at the same time. In the 3PI model, the electrons go through one solid phase, and transfer to the other solid phase which releases oxygen ions to balance the charge, resulting in a phase transformation. Apparently, as mentioned above, among the four three-phase interlines formed during the electrolytic process of titanium dioxide, only the three-phase interline of TiO/titanium/electrolyte matches the condition of 3PI. The TiO transforms to metal and connects with the newly formed titanium and electrolyte, resulting in the propagation of the three-phase interline. Namely, there are several interfaces and interlines proceeding at the same time in the electro-reduction of titanium oxide. Figure 10 shows the growth and propagation of the 3PIs in a quarter of a titanium oxide pellet that served as a cathode. As a result, the conclusion can be drawn that the electro-reduction process of the titanium dioxide is a complicated process with multiphase and multi-interface formation. Thus, this process could not be completely explained by the 3PI model.

Based on the above analysis, we can conclude that the electro-reduction of the titanium dioxide is a complicated multiphase and multi-interface process. It is assumed that the TiO<sub>2</sub> pellets first release a few oxygen ions as soon as the voltage is applied; thus, the pellets are able to react with the Ca<sup>2+</sup> and generate perovskite phases. This can be proven by the fact that the TiO<sub>2</sub> pellets cannot react with molten CaCl<sub>2</sub> without potential [25]. As a result, the volume of the experimental TiO<sub>2</sub> pellets first increase, then subsequently decrease after further electrolyzing, leaving cracks as shown in Fig. 1. In the end, the whole reaction pathway can be described as four steps. Figure 11 shows the details of the phase transition process. First, with the assistance of an electric field, a partial oxygen is removed from the cathode TiO<sub>2</sub> and reacts with calcium ions from the molten salt to form CaO. Second, the formed CaO reacts with the initial TiO<sub>2</sub> and generates perovskite phases. Third, the perovskite phase is electrolyzed to titanium suboxide and CaO. Finally, titanium suboxides are reduced to titanium mostly through the pathway of titanium suboxides → TiO → Ti. The mentioned reaction pathway is the dominating reaction route and is shown in blue in Fig. 11. In addition, the CaO formed intermediately may also be electrolyzed to calcium, then reacted with titanium suboxides to obtain titanium by calciothermic reduction. This process is marked by a dotted line in Fig. 11.

#### 4. CONCLUSION

In the present work, we demonstrate that the electro-chemical reduction of the TiO<sub>2</sub> in CaCl<sub>2</sub> is accompanied with the formation of perovskite phases rather than direct reduction to metal. The formation and decomposition of the intermediate perovskite phases are inevitable steps. Here are the main conclusions.

(1) During the electro-deoxidization of TiO<sub>2</sub>, the perovskite phases were generated quickly by the reaction between Ca<sup>2+</sup> from the calcium chloride salt and O<sup>2-</sup> released from TiO<sub>2</sub> with un-deoxygenated TiO<sub>2</sub> in the cathode. The perovskite phase is further electrolyzed to titanium suboxides with the proceeding of the electro-deoxidization.

(2) The electro-deoxidization process of TiO<sub>2</sub> in molten CaCl<sub>2</sub> is a complicated process including multiple phases and interfaces. Four main three-interlines exist, which are titanium

dioxide/perovskite/electrolyte, perovskite/titanium suboxides/electrolyte, titanium suboxides/TiO/electrolyte and TiO/titanium/electrolyte. The growth, propagation and extinction of these three-phase interlines are interacted on each other.

(3) The deoxidization rate of the whole process is primarily affected by the deoxidization rate of perovskite and titanium suboxides.

## ACKNOWLEDGEMENTS

The authors acknowledge gratefully the financial support from the National Natural Science Foundation of China (Grant No. 51674054 and Grant No. 51234010).

## References

1. K.S. Mohandas, *Trans. Inst. Min. Metall. C*, 122 (2013) 195.
2. T. Nohira, K. Yasuda, Y. Ito, *Nat. Mater.*, 2 (2003) 397.
3. K. Yasuda, T. Nohira, Y. Ito, *J. Phys. Chem. Solids*, 66 (2005) 443.
4. G.Z. Chen, D.J. Fray, T.W. Farthing, *Nature*, 407 (2000) 36.
5. P.K. Tripathy, M. Gauthier, D.J. Fray, *Metall. Mater. Trans. B*, 38 (2007) 893.
6. S. Wang, Y. Li, *J. Electroanal. Chem.*, 571 (2004) 37.
7. Q. Song, Q. Xu, X. Kang, J. Du, Z. Xi, *J. Alloy Compd.*, 490 (2010) 241.
8. T. Wu, X. Jin, X. Wei, X. Hu, D. Wang, G.Z. Chen, *Chem. Mater.*, 19 (2007) 153.
9. G.Z. Chen, E. Gordo, D.J. Fray, *Metall. Mater. Trans. B*, 35 (2004) 223.
10. E. Gordo, G.Z. Chen, D.J. Fray, *Electrochim. Acta*, 49 (2004) 2195.
11. M.J. Sang, H.S. Shin, S.H. Cho, J.M. Hur, S.L. Han, *Electrochim. Acta*, 54 (2009) 6335.
12. M.J. Sang, H.S. Shin, S.S. Hong, J.M. Hur, J.B. Do, S.L. Han, *Electrochim. Acta*, 55 (2010) 1749.
13. A. Cox, D.J. Fray, *J. Appl. Electrochem.*, 38 (2008) 1401.
14. S. Wang, G.M. Haarberg, E. Kvalheim, *J. Iron. Steel Res. Int.*, 15 (2008) 48.
15. G.Z. Chen, D.J. Fray, *J. Electrochem. Soc.*, 149 (2002) 455.
16. D.S.M. Vishnu, N. Sanil, L. Shakila, R. Sudha, K.S. Mohandas, K. Nagarajan, *Electrochim. Acta*, 159 (2015) 124.
17. R. Bhagat, D. Dye, S.L. Raghunathan, R.J. Talling, D. Inman, B.K. Jackson, K.K. Rao, R.J. Dashwood, *Acta Mater.*, 58 (2010) 5057.
18. K. Dring, R. Dashwood, D. Inman, *J. Electrochem. Soc.*, 152 (2005) 104.
19. C. Schwandt, D.J. Fray, *Electrochim. Acta*, 51 (2005) 66.
20. C. Schwandt, D.T.L. Alexander, D.J. Fray, *Electrochim. Acta*, 54 (2009) 3819.
21. D.T.L. Alexander, C. Schwandt, D.J. Fray, *Electrochim. Acta*, 56 (2011) 3286.
22. D.T.L. Alexander, C. Schwandt, D.J. Fray, *Acta Mater.*, 54 (2006) 2933.
23. G.Z. Chen, D.J. Fray, Understanding the electro-reduction of metal oxides in molten salts, Symposium of Recent Advances in Non-Ferrous Metals Processing, 2004 TMS Annual Meeting, Charlotte, USA, 2004, 881.
24. Y. Deng, D. Wang, X. Wei, X. Jin, X. Hu, G.Z. Chen, *J. Phys. Chem. B*, 109 (2005) 14043.
25. J. Mohanty, K.G. Mishra, R.K. Paramguru, B.K. Mishra, *Metall. Mater. Trans. B*, 43 (2012) 513.